PAPER • OPEN ACCESS

Simulation of edge cracking using shear GTN damage model during hot plate rolling of magnesium alloys

To cite this article: C C Zhao *et al* 2022 *IOP Conf. Ser.: Mater. Sci. Eng.* **1270** 012074

IOP Conf. Series: Materials Science and Engineering 1270 (2022) 012074 doi:10.1088/1757-899X/1270/1/012074

Simulation of edge cracking using shear GTN damage model during hot plate rolling of magnesium alloys

C C Zhao[1,2], J L Liu[1,2,3], Z X Li[1,2,3], R Jia[1,2], Z Q Huang[4] and T Wang[1,2,3,*]
[1] College of Mechanical and Vehicle Engineering, Taiyuan University of Technology, Taiyuan, 030024, P.R. China
[2] Engineering Research Center of Advanced Metal Composites Forming Technology and Equipment, Ministry of Education, Taiyuan, 030024, P.R. China
[3] TYUT-UOW Joint Research Center, Taiyuan University of Technology, Taiyuan, 030024, P.R. China
[4] School of Materials Science and Engineering, Taiyuan University of Science and Technology, Taiyuan, 030024, P.R. China
[*] Corresponding author, E-mail: twang@tyut.edu.cn

Abstract. Edge cracks are a more prominent problem during the rolling process of magnesium alloy sheets. The hexagonal structure of magnesium alloys and the product defects caused by the second phase impurities mixed in the sheets are the main causes of edge cracking. Conventional hot-rolled edge cracking simulations can only characterize the edge damage of the sheets numerically, however, the actual crack morphology is ignored. In this paper, the Gurson-Tvergaard-Needleman (GTN) damage model coupled with a continuous medium shear damage model was developed for improving the applicability of the model at low-stress triaxiality. Powell's “Dogleg” method was used in the numerical solution of the damage model instead of the traditional Newton-Raphson method and the Vumat subroutine was written for the finite element simulation by the stress return algorithm. The damage model parameters were calibrated by a shear specimen. The results showed a good agreement between the simulated crack morphology and the experiment.

1. Introduction

Magnesium alloys have a wide range of applications in aerospace and automotive industries due to their excellent characteristics such as low density and high strength [1,2]. However, due to the unique dense row hexagonal crystal structure of magnesium alloy, it is difficult to start the slip system in plastic forming, and it is very easy to produce edge cracks in the process of rolling production [3]. The study of the edge cracking behaviors of magnesium alloy during rolling will have guiding significance for its production.

A reasonable simulation prediction of edge cracking in magnesium alloy rolling will help to explain the causes of edge cracking in magnesium alloy rolling production. With the help of the finite element method (FEM), Ning et al. [4] established the criterion of edge cracking in magnesium alloy rolling by Cockcroft and Latham (C-L) criterion and concluded that the edge cracking in magnesium alloy originates from the maximum tensile stress at the edge of the sheet. Jia et al. [5] established the criterion of edge cracking in magnesium alloy rolling based on Freudenthal criterion, and it was considered that the edge crack was mainly related to the rolling temperature and rolling reduction. Although the above models can provide some solutions to the prediction of the edge crack of magnesium alloy rolling, for their mechanical models, the influences of hydrostatic stress, Lode

IOP Conf. Series: Materials Science and Engineering 1270 (2022) 012074 doi:10.1088/1757-899X/1270/1/012074

parameter, stress triaxiality, etc. on the material damage are not considered. It will lead to the critical damage value becoming the only variable for the prediction of edge cracking in magnesium alloy rolling. Another problem is that the prediction of edge cracks is all in the form of damage clouds based on finite elements, which do not simulate real cracks.

In this paper, to better predict the edge damage of magnesium alloy rolling, the GTN model based on the continuous medium damage factor containing was applied to the prediction of edge cracking in magnesium alloy rolling, the material damage parameters were identified by a shear specimen, and the simulation of edge cracking in magnesium alloy rolling was performed by the Vumat user subroutine of Abaqus finite element software.

2. Damage model

2.1. The original GTN model

The GTN model is based on the Gurson [6] model. The yield function of the GTN model can be expressed in the following form:

$$\phi = (\frac{\sigma_{eq}}{\sigma_y})^2 + 2q_1 f \cosh(\frac{3q_2\sigma_m}{2\sigma_y}) - 1 - (q_1 f^*)^2 \tag{1}$$

where σ_{eq} , σ_m and σ_y are the von Mises equivalent stress, hydrostatic stress, and flow stress respectively. q_1, q_2 denote the material damage constants, related to the second phase particles of the matrix. The variable f^* was introduced into the yield surface function of the model by Tvergarrd and Needleman [7] as the effective void volume fraction:

$$f^* = \begin{cases} f_c + \dfrac{1/q_1 - f_c}{f_f - f_c}(f - f_c) & f_c < f < f_f \\ 1/q_1 & f > f_f \end{cases} \tag{2}$$

where f_c and f_f denote the void volume fraction when void coalescence and material fracture respectively.

For the evolution of the void volume fracture, the GTN model takes into account the new voids nucleation and the void growth, which can be written as [8]:

$$\dot{f} = \dot{f}_n + \dot{f}_g \tag{3}$$

where $\dot{f}_n$ denotes the nucleation rate of new voids. Chu and Needle [9] related the evolution of $\dot{f}_n$ to the equivalent matrix plastic strain and can be expressed as:

$$\begin{cases} \dot{f}_n = A_n \dot{\varepsilon}_p^{eq} \\ A_n = \dfrac{f_N}{S_N\sqrt{2\pi}} \exp\left[-\dfrac{1}{2}\left(\dfrac{\varepsilon_p^{eq} - \varepsilon_N}{S_N}\right)^2\right] \end{cases} \tag{4}$$

where ε_p^{eq} is equivalent matrix plastic strain and f_N denotes the volume fraction of void nucleation particles. ε_N and S_N denote the mean equivalent matrix plastic strain of nucleation and the standard deviation of the normal distribution. Correspondingly, the equation for the void growth can be written as:

$$\dot{f}_g = (1 - f)\dot{\varepsilon}_m \tag{5}$$

where $\dot{\varepsilon}_m$ denotes the plastic strain rate due to hydrostatic stress.

2.2. Extended GTN model

Zhou et al. [10] introduced a continuous medium shear damage factor to the GTN damage model, and the new yield surface function could be expressed as:

$$\phi = (\frac{\sigma_{eq}}{\sigma_y})^2 + 2q_1 f \cosh(\frac{3q_2\sigma_m}{2\sigma_y}) - 1 - (q_1 f^* + D_s)^2 + 2D_s \tag{6}$$

Where $q_1 f^* + D_s$ is the total damage value. When the total damage value becomes unity, the material is considered to lose its carrying capacity completely. The variable D_s is the shear damage factor, which evolution equation can be written as:

$$D_s = \varphi(\theta,\eta)(\frac{\varepsilon_p^{eq}}{\varepsilon_f})^n \tag{7}$$

where n is the softening factor of material fracture and ε_f denotes the critical fracture equivalent plastic strain of material. $\varphi(\theta,\eta)$ is a function of the Lode angle and the stress triaxial, which can be expressed as:

$$\varphi(\theta,\eta) = \begin{cases} g_0\eta & (\eta \geq 0) \\ g_0(1-T_k) + T_k & (\eta < 0) \end{cases} \tag{8}$$

where η is the stress triaxial and constant T_k is the weight factor when the stress triaxial is negative. The expression of the weight function g_0 is not unique. In this work, the weight function was taken to be the same as Xue et al. [11], which can be written as: $g_0 = 1 - \frac{6|\theta|}{\pi}$. Where θ is the Lode angle. Eq. (7) and Eq. (8) show that the original GTN damage model dominates when the matrix is in a high stress triaxiality state. Correspondingly, When the matrix is in a negative stress triaxiality state, the continuous media damage model will dominate and characterize material damage by the evolution of D_s.

The critical fracture equivalent plastic strain of material is not constant, but changes with the change of stress state. To avoid the damage factor D_s growing too fast when the matrix is in a negative stress triaxiality state and to improve the accuracy of shear damage, Wu et al. [12] considered the fracture strain as a function of stress triaxiality based on the research of Lou et al. [13] and Bai and Wierzbicki [14], which could be expressed as:

$$\overline{\varepsilon_f} = \begin{cases} \varepsilon_f & \eta > 0 \\ \varepsilon_f \left[1 - q_0 \ln(1 - \frac{\eta}{\eta_{lim}})\right] & \eta_{lim} < \eta < 0 \\ +\infty & +\infty \end{cases} \tag{9}$$

where q_0 is a material constant and η_{lim} is the critical stress triaxiality.

According to the derivation of Lou et al. [13], the critical stress triaxiality should obey the following function:

$$f(\eta,\mu_\alpha,C) = \eta_{lim} + \frac{(3-\mu_\alpha)}{3\sqrt{\mu_\alpha^2 + 3}} + C \tag{10}$$

where μ_α is the Lode parameter. Based on the suggested value of C =1/3 given by Wu et al. [12], we can calculate $\eta_{lim} \approx$-0.9107 when $\mu_\alpha = 0$, which indicates that when the stress triaxiality is less than -0.9107, the shear damage factor D_s will no longer grow.

2.3. Numerical method
The equations to be solved for the extended GTN damage model are as follows:

$$\begin{cases} F_1 = (\dfrac{\sigma_{eq}}{\sigma_y})^2 + 2q_1 f^* \cosh(\dfrac{3q_2\sigma_m}{2\sigma_y}) - 1 - (\mathrm{q_1 f^*} + \mathrm{D_s})^2 + 2D_s = 0 \\ F_2 = \dfrac{\partial F_1}{\partial \sigma_{eq}} - \dfrac{\partial F_1}{\partial \sigma_m} = 0 \\ F_3 = \dfrac{\sigma_{eq}\varepsilon_{eq} + \sigma_m \varepsilon_m}{(1-f)\sigma_y} - \varepsilon_p^{eq} = 0 \\ F_4 = f - f_0 - f_n - f_g = 0 \end{cases} \tag{11}$$

where F_1 is the yield surface function of the modified GTN damage model, when F_1<0 means the elastic stage, F_1>0 means the plastic stage. F_2 denotes the associated flow rule equation, considering the growth rate of plastic strain due to von Mises equivalent stress is the same as the growth rate of plastic strain due to hydrostatic stress. F_3 denotes equivalent plastic strain solved by equivalence of macroscopic plastic work and microscopic plastic work. F_4 denotes solving the void volume fraction.
The research of Shterenlikht et al. [15] showed that Newton's method may not converge at all, or converge to a local minimum, but the “Dogleg” numerical iteration method did not have this problem. In this work, Eq. (13) was solved using "Dogleg" method, and the stress return algorithm proposed by Aravas [16] was compiled into the Vumat subroutine. The program flowchart is shown in figure 1.

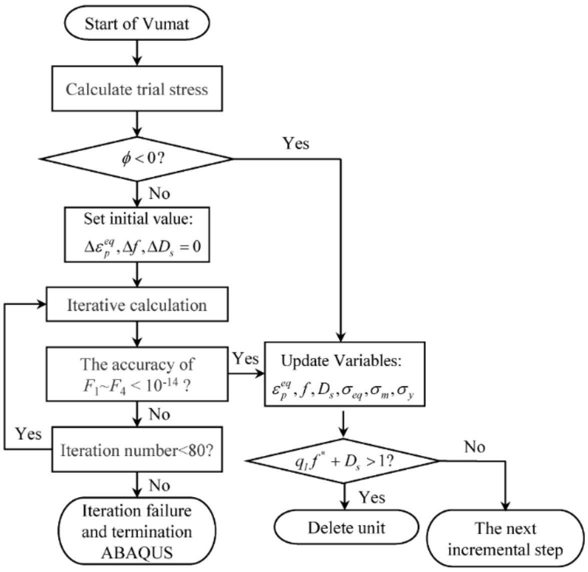

Figure 1. Vumat subroutine flowchart.

3. Results and discussion

3.1. Hot rolling test of magnesium alloy
The experimental material was a 2-mm-thick AZ31B magnesium alloy industrial hot rolled formed sheet and small sheets were cut along the rolling direction of the hot-rolled plate to a size of 60 mm ×100 mm ×2 mm. The magnesium alloy sheets were preheated (at 300 °C and held for 20 min) and then rolled immediately. Specific process parameters are shown in table 1.

Table 1. Rolling process parameters.

Roller diameter (mm)	Roll speed (rad/s)	Rolling reduction (%)
150	1	35

3.2. Material and damage model parameters

The flow stress model proposed by Serajzadeh et al. [17] was introduced to describe the isotropic hardening behavior of material:

$$\sigma_y = [\sigma_s^2 + (\sigma_0^2 - \sigma_s^2)\exp(-\Omega_\varepsilon \varepsilon_p^{eq})]^{1/2} \tag{12}$$

where σ_s is the steady-state flow stress representing the balance between work hardening and dynamic recovery. σ_0 is the yield stress of the material and Ω_ε is the softening factor. The elastic-plastic property of the material was determined via a standard uniaxial tensile test as listed in Table 2.

Table 2. Material elastic-plastic parameters.

E (GPa)	μ	σ_s (MPa)	σ_0 (MPa)	Ω_ε
20	0.35	238	129	7

To identify damage parameters of AZ31B magnesium alloy, the values of q_1 and q_2 suggested by Tvergaard [18] were adopted in the current research. In addition, the f_N, f_0 parameters of the AZ31B magnesium alloy identified by scanning electron microscopy (SEM) by Henseler et al. [19] were quoted. The remaining parameters were identified using the tensile test.

A shear specimen of magnesium alloy was prepared, and the dimension is shown in figure 2(a). The shear specimen was preheated (at 300 °C and held for 20 s) and then tested on an electronic universal mechanical test machine to obtain the load-displacement curve.

As shown in figure 2(b), a shear specimen of the same size model was built in Abaqus. The mesh size was gradually increased from the middle area of the shear specimen to the outside using the neutral axis algorithm, where the global approximate mesh size was 0.8, and the mesh type was C3D8R. As shown in figure 3(a), the Vumat subroutine was embedded in Abaqus/Dynamical-Explicit for simulated tensile experiment, and then the simulated value of the load-displacement curve was fitted to the actual value by changing the damage parameters. The final values of the damage parameters obtained are shown in Table 3 and Table 4(the result of the curve fit is shown in figure 3(b)).

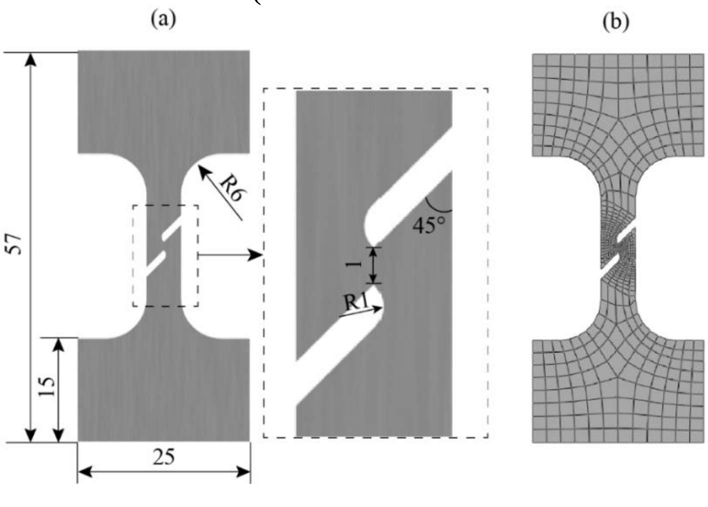

Figure 2. Damage parameters test experiment: (a) Dimension of the specimen; (b) The shear specimen model in Abaqus.

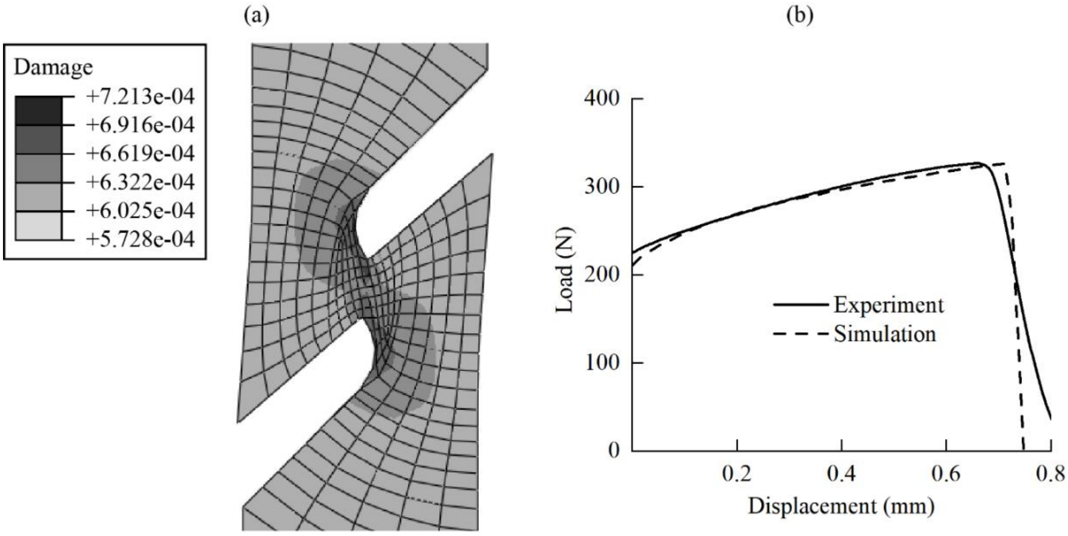

Figure 3. Simulated results of the damage parameters test experiment: (a)Simulation of shear specimen; (b)Comparison on load-displacement curve of experiment and simulation results.

Table 3. The GTN model parameters.

q_1	q_2	ε_N	S_N	f_N	f_0	f_c	f_f
1.5	1	0.55	0.0246	0.011	0.0004	0.0018	0.01

Table 4. The shear damage parameters.

ε_f	n	T_k	q_0	η_{lim}
0.55	5	0.5	1.25	-0.9107

3.3. Rolled edge crack simulation

The finite element simulation of the magnesium alloy rolling was built in Abaqus/Dynamical-Explicit, as shown in figure 4. To improve the computational efficiency, 1/4 volume of the actual magnesium alloy sheet volume (100 mm ×60 mm ×2 mm) was taken to build the sheet model.

At the beginning of rolling, the sheet had an initial speed of 10 mm/s and the roller had a constant speed of 1rad/s. The penalty contact method was adopted to simulate the contact between the sheet and roller and Coulomb's law was applied to characterize the friction between them. The friction coefficient between sheet and roller was 0.5.

figure 5 shows the sheet meshes adopted in the simulation. Two sizes of mesh were designed for the edge and centre areas of the sheet and were connected by transition meshes. The mesh type was C3D8R and the mesh size was 0.25 mm in the edge area and 0.5 mm in the centre area.

Figure 6 and figure 7 show the simulated and experimental results of edge cracking in magnesium alloy rolling respectively. The results show a gradual expansion of the crack from the edge area to the centre of the sheet and the simulated crack morphology is similar to the experimental results.

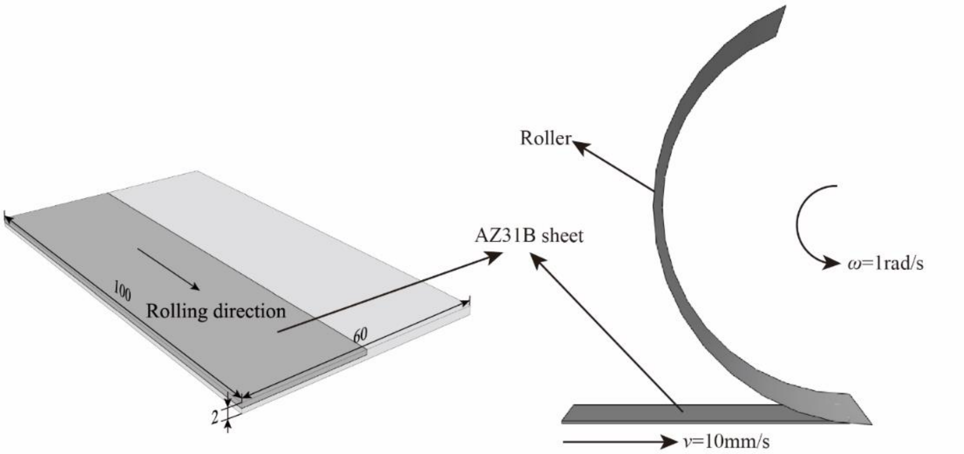

Figure 4. Rolling model in Abaqus/Dynamical-Explicit.

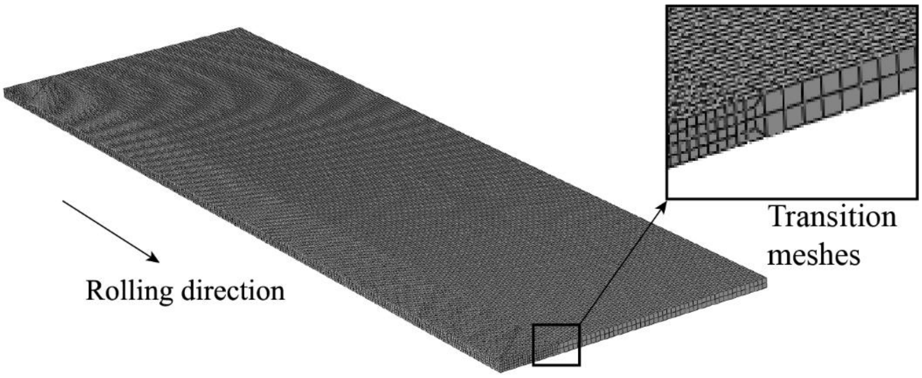

Figure 5. Meshes division of the sheet.

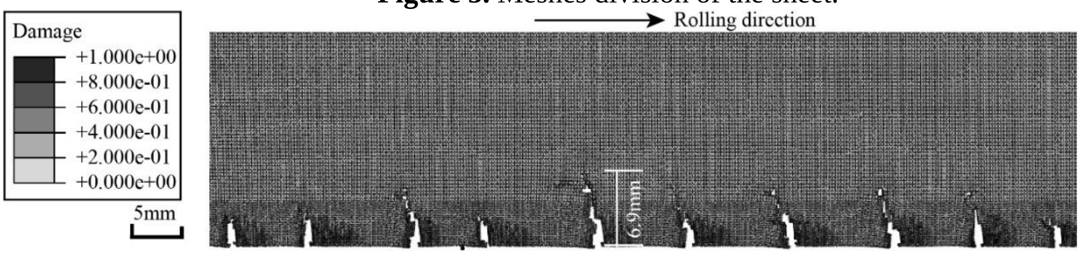

Figure 6. Rolling simulation results.

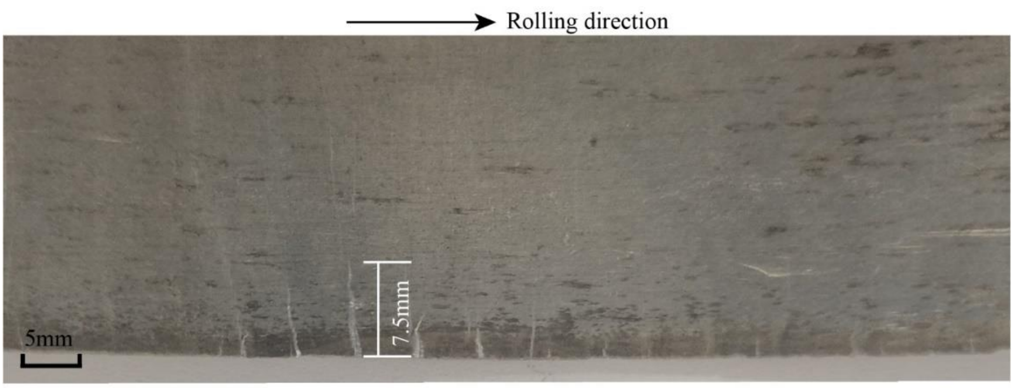

Figure 7. Rolling experiment results.

IOP Conf. Series: Materials Science and Engineering 1270 (2022) 012074 doi:10.1088/1757-899X/1270/1/012074

4. Conclusion

The traditional model for predicting edge cracks in rolled AZ31B magnesium alloy relied on damage value clouds. In this paper, the modified GTN model was compiled into a Vumat subroutine embedded in Abaqus/Dynamical-Explicit finite element software to effectively predict the edge crack morphology of AZ31B magnesium alloy, which provided a new way to accurately predict the edge crack of magnesium alloy rolling. In addition, the maximum crack depth of simulation was 6.9 mm, which was in good agreement with the experimental result of 7.5 mm.

References

[1] Tian J, Lu H, Zhang W, Nie H, Shi Q, Deng J, Liang W and Wang L 2021 An effective rolling process of magnesium alloys for suppressing edge cracks: Width-limited rolling *Journal of Magnesium and Alloys* DOI:10.1016/j.jma.2021.01.007

[2] Li S, Han J, Wang T, Liu Y, Fu X and Liu J 2020 Interfacial evolution and mechanical property of AZ31BMg/5052Al clad plate manufactured by corrugated + flat rolling technique *Procedia Manufacturing* **50** 148–52

[3] Nie H, Zheng L, Tian J and Liang W 2021 Edge crack behavior and strengthening mechanism of width-limited rolled AZ31 magnesium sheet with large reduction *Journal of Mechanical Engineering* **57** 146–53

[4] Ning F, Jia W, Hou J, Chen X and Le Q 2018 Construction of edge cracks pre-criterion model based on hot rolling experiment and simulation of AZ31 magnesium alloy *Mater. Res. Express* **5** 056528

[5] Jia W, Ma L, Jiao M, Le Q, Han T and Che C 2020 Fracture criterion for predicting edge-cracking in Hot rolling of twin-roll casted AZ31 Mg alloy *Journal of Materials Research and Technology* **9** 4773–87

[6] Gurson A L 1977 Continuum theory of ductile rupture by void nucleation and growth: part i—yield criteria and flow rules for porous ductile media *J. Eng. Mater. Technol.-Trans. ASME* **99** 297–300

[7] Tvergaard V and Needleman A 1984 Analysis of the cup-cone fracture in a round tensile bar *Acta Metallurgica* **32** 157–69

[8] Needleman A and Tvergaard V 1984 An analysis of ductile rupture in notched bars *Journal of the Mechanics and Physics of Solids* **32** 461–90

[9] Chu C C and Needleman A 1980 Void nucleation effects in biaxially stretched sheets *Journal of Engineering Materials and Technology* **102** 249

[10] Zhou J, Gao X, Sobotka J C, Webler B A and Cockeram B V 2014 On the extension of the Gurson-type porous plasticity models for prediction of ductile fracture under shear-dominated conditions *Int. J. Solids. Struct.* **51** 3273–91

[11] Xue L 2008 Constitutive modeling of void shearing effect in ductile fracture of porous materials *Eng. Fract. Mech.* **75** 3343–66

[12] Wu H, Xu W, Shan D and Jin B C 2019 An extended GTN model for low stress triaxiality and application in spinning forming *J. Mater. Process. Tech.* **263** 112–28

[13] Lou Y, Yoon J W and Huh H 2014 Modeling of shear ductile fracture considering a changeable cut-off value for stress triaxiality *International Journal of Plasticity* **54** 56–80

[14] Bai Y and Wierzbicki T 2008 A new model of metal plasticity and fracture with pressure and Lode dependence *International Journal of Plasticity* **24** 1071–96

[15] Shterenlikht A and Alexander N A 2012 Levenberg–Marquardt vs Powell's dogleg method for Gurson–Tvergaard–Needleman plasticity model *Computer Methods in Applied Mechanics and Engineering* **237–240** 1–9

[16] Aravas N 1987 On the numerical integration of a class of pressure-dependent plasticity models *Int. J. Numer. Meth. Engng.* **24** 1395–416

[17] Serajzadeh S and Karimi Taheri A 2003 Prediction of flow stress at hot working condition *Mechanics Research Communications* **30** 87–93

[18] Tvergaard V 1982 On localization in ductile materials containing spherical voids *Int. J. Fract.* **18** 237–52
[19] Henseler T, Osovski S, Ullmann M, Kawalla R and Prahl U 2020 GTN model-based material parameters of AZ31 magnesium sheet at various temperatures by means of SEM in-situ testing *Crystals* **10** 856

Acknowledgments
This work was financially supported by the National Natural Science Foundation of China (52075359), China Postdoctoral Foundation (2020M670710) and Fundamental Research Program of Shanxi Province (20210302124115).